

Petrology and geochemistry of monchiquites from Tchircotché (Garoua rift, north Cameroon, Central Africa)

I. Ngounouno¹, B. Déruelle², R. Montigny³, and D. Demaiffe⁴

¹Département des Sciences de la Terre, Faculté des Sciences,
Université de Ngaoundéré, Ngaoundéré, Cameroun

²Laboratoire de Magmatologie et Géochimie Inorganique et Expérimentale,
CNRS-UMR 7047, Université Pierre et Marie Curie, et
IUFM Académie de Versailles, Paris, France

³Ecole et Observatoire de Physique du Globe, URA CNRS 323,
Université Louis Pasteur, Strasbourg, France

⁴Laboratoire de Géochimie Isotopique, Université Libre de Bruxelles,
Bruxelles, Belgique

Received October 14, 2002; revised version accepted October 1, 2004

Published online December 7, 2004; © Springer-Verlag 2004

Editorial handling: *J. Foden*

Summary

Dykes of Cenozoic age (37.5 ± 2.3 Ma) crop out in the Tchircotché area (Garoua rift, north Cameroon). They consist of a lamprophyric (monchiquite) series with diopside, subsilicic kaersutite and apatite phenocrysts, Ba–Ti-rich biotite microphenocrysts and Cr-diopside xenocrysts scattered in a matrix of analcitic composition containing oligoclase, albite and sanidine microlites and carbonate ocelli.

Major and trace element distributions are interpreted in terms of crystal fractionation of olivine, clinopyroxene, amphibole and Fe–Ti oxides. The Tchircotché monchiquites show a relatively restricted range of initial $^{87}\text{Sr}/^{86}\text{Sr}$ ratio (0.70366–0.70387), of ϵ_{Nd} values (+2.5 to +2.7), and rare earth element patterns similar to those of the least differentiated basalts of the Cameroon Line. This supports a common magma source region. This mantle source is infra-lithospheric and is strongly enriched in incompatible elements (light REE, Zr, Sr, Ba) probably transported by volatile- and halogen-rich fluids. The monchiquites appear to be derived by low degrees of partial melting as attested by steep REE patterns and high contents of other incompatible elements, suggesting the presence of residual garnet in the source. Several lines of evidence support the occurrence of phlogopite in the source region of Tchircotché lamprophyre magma.

Introduction

The first comprehensive review on lamprophyres has been given by *Rock* (1991). More recently, a new classification scheme has been proposed (*Woolley et al.*, 1996). Three major types of lamprophyres are described worldwide: alkaline lamprophyres (AL), ultramafic lamprophyres (UML) and calc-alkaline lamprophyres (CAL). They form localized dike-swarms emplaced in different tectonic settings but often related to an extensional environment. Despite the attention paid to lamprophyres these last years, many aspects of their genesis are poorly understood. Furthermore, the nature and composition of their volatile-rich mantle sources are still debated and subject of controversies.

All the petrogenetic and geochemical data suggest that the lamprophyric magmas are issued from low degrees of partial melting of an upper mantle source at a depth of 100–150 km (*Rock*, 1991). These magmas usually have very high concentrations of volatiles (F, CO₂, H₂O) and incompatible trace elements (light REE, Zr, Sr, Ba). It has been proposed that these high volatile contents result either from a previously volatile and incompatible element-rich mantle source (*Delor and Rock*, 1991; *Wu and Berg*, 1992; *Ulrych et al.*, 1993; *Hoch*, 1999) or from CO₂–H₂O–F fluid-rich metasomatism (*McKenzie*, 1989; *Maury et al.*, 1992). The differentiation of the alkaline lamprophyre series is still highly debated. A number of hypotheses have been put forward to explain the genesis of the distinct members of the group (see *Rock*, 1991). Fractionation of pyroxene and amphibole with increasing fugacity of CO₂ and H₂O in continuously replenished fractionating magma chambers has been advocated (*Clarke et al.*, 1983; *Jelinek et al.*, 1989; *Mitchell et al.*, 1991).

Monchiquites commonly occur in alkali basalt provinces. Volumes of monchiquite are extremely low compared to those of basalts. They have even been said to be basalts modified by addition of volatile components (*Wimmenauer*, 1973). Experiments indicate that monchiquites may derive from hydrous melts of basaltic to nephelinitic compositions, as H₂O enhances the stability of hydrous minerals (amphibole, mica) and decreases the stability of plagioclase (*Rock*, 1987).

The main textural and paragenetic features of the Tchircotché rocks include: 1) a porphyritic texture with high Al–Ti clinopyroxene, kaersutite, olivine, apatite, and biotite phenocrysts; 2) occurrence of numerous ocelli rich in carbonate and 3) the coexistence of mafic minerals and analcite with alkali feldspars. All the above characteristics are restricted to rocks of the lamprophyre clan (*Rock*, 1991; *Woolley et al.*, 1996). Based on their major element composition (Fig. 2), the Tchircotché lamprophyres belong to the alkali type rather than to the ultramafic one. Petrographically they can be called “monchiquites”.

They are associated to the alkaline lava series of the Garoua rift. The monchiquites are exposed at the intersection between the Garoua rift (N120–N130° E) and Cameroon Line (N30° E) geostructures. The alkaline volcanism of the Cameroon Line is now well known although the origin of the basaltic magma (infra-lithospheric: *Déruelle et al.*, 1991; *Ngounouno et al.*, 2000, 2003; lithospheric: *Halliday et al.*, 1988, 1990) is still highly debated. This work presents the first petrographic and geochemical data on monchiquites along the Cameroon Line with the aim to establish if there is, or not, a relationship with alkali basalt magma sources.

Geological and tectonic settings

The Benue trough (Fig. 1) is a huge intracontinental rift, constituting the western part of the Mid-African Rift System, which propagates far inside Africa (*Kampunzu and Popoff*, 1991; *Guiraud and Bosworth*, 1997). It extends northwards into the Gongola branch (Nigerian part of the Upper Benue valley) and eastwards into the Yola branch. The Garoua rift is the N120° E–130° E propagation of the Yola branch in Cameroon and is limited by strike-slip faults. The main stage of rifting occurred during Neocomian to Lower Aptian times (*Benkhelil*, 1988). Subsidence during Aptian and Albian favoured the accumulation of voluminous conglomerates and sandstones (up to 5000 m thick, *Elf-Serepca*, unpublished data) which were folded during a regional Santonian compression (*Guiraud*, 1993; *Ngounouno et al.*, 1997b) and faulted during the Cenozoic. The monchiquite dykes intruded the sandstones metamorphosed into quartzites at their contacts. The dykes are half-meter to one meter thick, and are steeply dipping (>70°), with directions between N70° E and N135° E.

Numerous interpretations have been given to explain the formation of the Cameroon Line (for a comprehensive review, see *Déruelle et al.*, 1991). The most widely accepted structural explanation is that the Cameroon Line is due to the rejuvenation of a Pan-African N70° E fracture zone at the beginning of the opening of the Atlantic Ocean (*Moreau et al.*, 1987). More recently, the Cameroon Line has been distinguished from a rift system, and is considered as a “hot line” resulting from lithospheric cracks (N30° E) tapping a sublithospheric mantle (*Déruelle et al.*, 1998). The hot line hypothesis has been supported by deep-imaging seismic and gravity study on offshore Cameroon Line (*Meyers et al.*, 1998) and recent geochemical studies on Bambouto, Oku and Adamawa (*Marzoli et al.*, 1999, 2000). Whether or not the volcanism of the Cretaceous Garoua rift is related to that of the Cameroon Line is still debated. Nevertheless, the volcanism (27–35 Ma) of the Kapsiki plateau (200 km north of the Garoua rift) has been recently considered as the northernmost volcanic zone of the Cameroon Line (*Ngounouno et al.*, 2000) and it is therefore possible that the volcanism of the Garoua rift also belongs to the Cameroon Line.

Analytical procedures

The main mineral phases of the Tchircotché monchiquites have been analyzed by CAMEBAX electron microprobe at Université Pierre et Marie Curie, Paris. Table 1 shows the representative analyses of: – clinopyroxene (iron recalculated after *Droop* (1987) and classification after *Morimoto* (1989); 15 kV, 40 nA, 20 s by element except Ti: 30 s) – amphibole (iron recalculated after *Leake et al.*, 1997; 15 kV, 40 nA, 15 s by element except Ca and Ti: 20 s, Fe and Mn: 25 s, and F and Cl: 30 s) – biotite (5 kV, 10 nA, 10 s by element) – Ti-magnetite and ilmenite (iron recalculated after *Stormer*, 1983; 20 kV, 40 nA, 40 s by element except Al and Cr: 30 s) – apatite (iron recalculated as Fe³⁺; 15 kV, 10 nA, 15 s by element except REE: 60 s). The program of correction is from “PAP” (*Pouchou and Pichoir*, 1991).

Chemical compositions of Tchircotché monchiquites (Table 2) have been obtained by ICP and ICP-MS (CNRS, CRPG, Nancy); details about the analytical procedure can be found in *Carignan et al.* (2001).

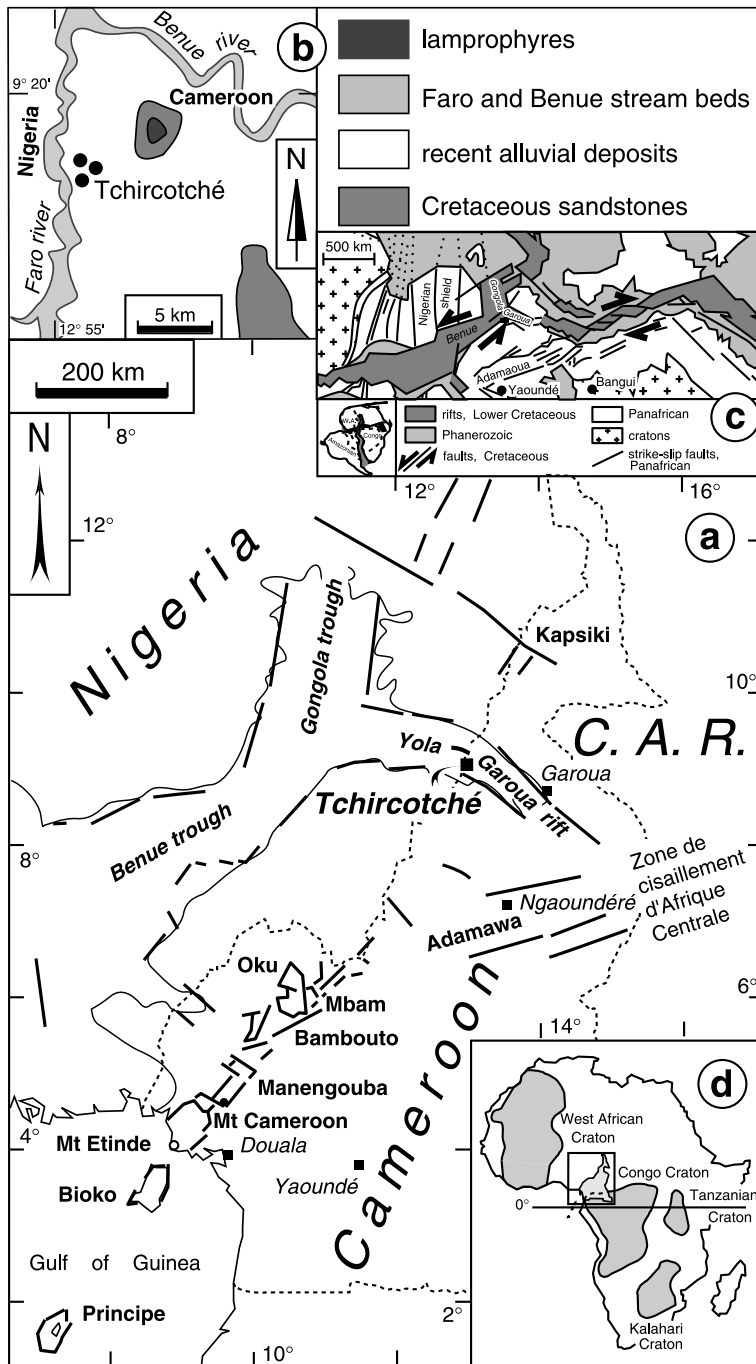


Fig. 1. **a** Location of the Tchircotché monchiquite dykes in the Garoua rift. The Cameroon Line (a succession of horsts and grabens) and the main other horsts and grabens are also indicated (after *Déruelle et al.*, 1991); **b** geological sketch map of the Tchircotché area (after *Ngounouno*, 1993); **c** West and Central African Rift System (after *Ngounouno et al.*, 2001); **d** Location of Fig. 1a in Africa (cratons, after *Kampunzu and Popoff*, 1991)

UML	Ultramafic lamprophyres
AL	Alkaline lamprophyres
CAL	Calc-alkaline lamprophyres

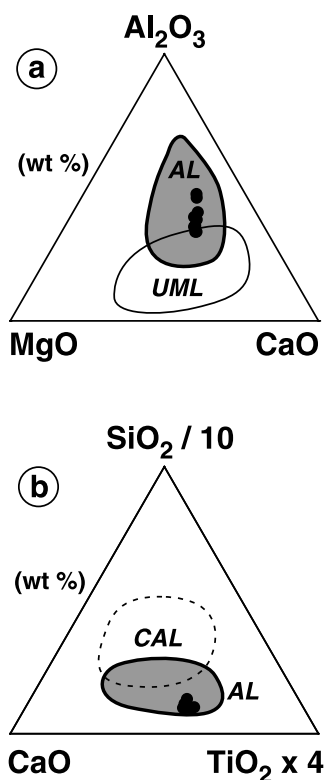


Fig. 2. The Tchircotché monchiquites in the discriminating graphs of *Rock* (1987)

For K–Ar ages, the analytical procedure, which is fully described elsewhere (*Bonhomme et al.*, 1975; *Montigny et al.*, 1988), is summarized below. Potassium content is determined by flame photometry with a lithium internal standard. Argon is extracted in a heat-resistant glass vacuum apparatus and determined by isotope dilution (^{38}Ar as a tracer) using a MS20 mass-spectrometer. All samples are measured in the static mode. The set of constants recommended by *Steiger and Jäger* (1977) is used for age calculation. Quoted uncertainties represent estimates of analytical precision at one standard deviation. They are calculated after the procedure given by *Cox and Dalrymple* (1967).

Samples for Rb–Sr and Sm–Nd isotopic analyses were dissolved in mixed HF–HNO₃ (10:1) acid mixture; chemical separation was carried out by cation-exchange chromatography; blanks were <1 ng. Sr and Nd isotopic ratios were measured on a VG Sector 54 multicollector thermal ionisation mass spectrometer (Univ. Libre de Bruxelles). Replicate analyses of the MERCK Nd standard gave an average $^{143}\text{Nd}/^{144}\text{Nd}$ value of 0.512742 ± 8 (normalized to $^{146}\text{Nd}/^{144}\text{Nd} = 0.7219$), and measurements of NBS 987 Sr yielded an average $^{87}\text{Sr}/^{86}\text{Sr}$ value of 0.710247 ± 7 (normalized to $^{86}\text{Sr}/^{88}\text{Sr} = 0.1194$). Epsilon Nd values were

Table 1. Representative CAMEBAX microprobe chemical analyses of minerals from Tchircotché monchiquites. Ph phenocryst; mph microphenocryst; m microcline; c core; r rim

Rock sample (wt%)	1		4		2		4		2		2		2		2	
	ph, c	ph, r	ph, c	ph, r	ph, c	ph, c	ph, c	ph, c	ph, c	ph, c	ph, c	ph, c	ph, c	ph, c	ph, c	ph, c
SiO ₂	44.65	44.04	54.05	54.05	39.51	34.39	35.26	35.26	59.68	66.13	59.68	66.13	59.68	66.13	59.68	66.13
TiO ₂	3.51	4.20	0.22	0.22	6.59	9.81	7.67	7.67								
Al ₂ O ₃	8.17	8.52	0.62	0.62	12.99	16.68	13.61	13.61	25.20	19.18	25.20	19.18	25.20	19.18	25.20	19.18
Cr ₂ O ₃	0.01	0.03	0.25	0.25						0.11		0.11				
FeO*	7.17	6.83	2.75	2.75	9.82	11.82	18.15	18.15	0.39	0.38	0.39	0.38	0.39	0.38	0.39	0.38
MnO	0.08	0.04	0.03	0.03	0.15	0.18	0.18	0.18								
MgO	12.14	11.81	17.06	17.06	13.20	14.11	11.35	11.35								
CaO	22.79	23.06	24.45	24.45	12.30	0.05	0.06	0.06	5.75	0.10	5.75	0.10	5.75	0.10	5.75	0.10
Na ₂ O	0.55	0.53	0.20	0.20	2.12	0.78	0.55	0.55	7.43	3.51	7.43	3.51	7.43	3.51	7.43	3.51
K ₂ O					1.57	7.96	8.55	8.55	1.17	11.59	1.17	11.59	1.17	11.59	1.17	11.59
P ₂ O ₅																
SrO						3.97	0.16	0.16								
BaO							0.04	0.04	0.02							
Ce ₂ O ₃																
La ₂ O ₃																
F					0.26	0.70	0.72	0.72								
Cl					0.03	0.01	0.03	0.03								
Sum	99.08	99.07	99.63	99.63	98.26	99.74	95.41	95.41	99.82	100.91	99.82	100.91	99.82	100.91	99.82	100.91
<i>recalculated</i>																
Fe ₂ O ₃	4.59	3.89	0.69	0.69												
FeO	3.04	3.33	2.13	2.13	12.18											
Sum	99.54	99.46	99.70	99.70	100.62											

(continued)

Table 2. Chemical compositions of Tchircotché monchiquites

Sample	6	8	9	4	1	7	3	5	2
(wt%)									
SiO ₂	38.67	37.62	37.78	37.84	38.37	37.84	38.51	40.17	41.00
TiO ₂	4.94	5.00	5.05	5.04	4.74	5.07	4.37	3.87	3.87
Al ₂ O ₃	11.83	11.57	11.89	12.42	12.96	12.88	13.36	14.00	14.67
Fe ₂ O ₃ *	14.31	14.68	14.91	14.94	14.00	15.17	12.88	11.38	11.14
MnO	0.17	0.17	0.17	0.19	0.17	0.20	0.17	0.19	0.20
MgO	8.14	7.91	7.75	7.74	7.00	7.00	6.25	5.09	4.84
CaO	15.26	14.71	14.01	14.63	13.86	13.17	13.21	11.19	11.19
Na ₂ O	2.41	1.75	1.43	2.12	1.77	1.95	2.29	2.45	2.11
K ₂ O	1.12	1.46	1.67	1.41	1.97	2.00	2.37	3.20	3.27
P ₂ O ₅	0.77	0.79	0.83	0.86	0.89	1.01	0.88	0.88	0.91
I.L.*	2.04	2.61	2.80	2.41	3.86	3.00	5.23	5.80	6.42
CO ₂	(0.21)	(0.73)	(0.49)	(0.31)	(0.82)	(0.75)	(2.52)	(2.60)	(2.61)
Total	99.66	98.27	98.29	99.60	99.59	99.29	99.52	98.22	99.62
CIPW norm									
Or			3.84		7.73	8.60	14.01	18.91	19.32
Ab							4.89	11.00	13.64
An	18.15	19.40	21.09	20.21	21.60	20.49	19.18	17.75	20.90
Lc	5.19	6.77	4.73	6.53	3.07	2.54			
Ne	11.05	8.02	6.55	9.72	8.11	8.94	7.85	5.28	2.28
Di	41.28	35.38	32.26	36.23	29.27	27.20	20.00	12.65	9.88
Ol	6.56	8.43	9.36	8.02	8.66	10.01	10.05	9.92	10.26
Mt	4.15	4.26	4.32	4.33	4.06	4.39	3.74	3.31	3.23
Ilm	9.38	9.50	9.59	9.57	9.00	9.63	8.30	7.35	7.35
Ap	1.77	1.82	1.91	1.98	2.05	2.33	2.03	2.03	2.10
Cc	0.48	1.66	1.11	0.70	1.86	1.71	5.73	5.91	5.94
(ppm)									
Be	2.4	2.5	2.4	2.7	2.5	2.6	2.5	2.5	2.7
Rb	24	32	34	30	39	45	42	78	53
Sr	912	845	885	1314	1186	1094	1297	1407	1542
Ba	443	1046	848	894	766	915	907	1410	7914
V	434	460	421	461	393	455	384	331	317
Cu	85	88	92	89	89	103	79	6	57
Cr	61	59	48	52	34	52	30	26	19
Co	47	47	33	47	33	48	34	33	25
Ni	75	72	64	68	51	67	48	42	30
Sc	36.2	34.7	33.5	33.2	28.7	28.1	25.3	19.3	18.4
Zn	103	104	107	110	110	117	104	105	114
Ga	21	18	5	28	20	17	25	21	37
Y	31	32	32	32	33	33	32	33	33
Zr	373	368	375	373	392	394	405	426	450
Nb	86	71	68	82	84	93	99	132	119
La	61.51	59.60	63.68	63.65	69.05	74.73	76.84	86.91	94.36
Ce	139	133	140	145	140	159	164	179	187
Nd	75.4	71.2	72.7	71.5	70.3	79.9	73.9	82.6	85.2
Sm	14.7	14.5	14.7	14.0	13.4	15.3	13.4	14.8	15.8
Eu	4.31	4.09	4.13	3.99	3.76	4.38	3.75	4.42	4.53
Gd	10.8	10.2	10.5	11.9	10.5	11.2	10.7	10.7	11.6
Dy	7.1	6.7	6.9	6.8	6.6	7.0	6.5	6.8	7.5
Er	2.7	2.6	2.6	2.8	2.7	2.7	2.7	2.7	3.5
Yb	1.87	1.88	1.94	1.77	1.68	2.00	1.69	2.04	2.23
Lu	0.27	0.26	0.26	0.33	0.30	0.28	0.29	0.30	0.40
Th	14	13	8	15	9	13	17	22	15

calculated assuming $^{147}\text{Sm}/^{144}\text{Nd} = 0.1967$ and $^{143}\text{Nd}/^{144}\text{Nd} = 0.512638$ for CHUR (see *Ashwal et al., 2002* for a detailed description of the procedure).

Results

Sample description

The Tchircotché lamprophyres belong to the alkaline lamprophyre group (Fig. 2). They do not contain any feldspar phenocrysts and are diopside-rich, they are thus typical monchiquites. Their texture is porphyritic with phenocrysts of clinopyroxene (vol dominant phase), amphibole, olivine, apatite and occasionally biotite. The mineral proportions have been determined (*Ngounouno, 1993*) by point counting (3500 points). Clinopyroxene phenocrysts (up to 1 cm in length) are oscillatory zoned, lilac-brownish (indicating high Ti contents), and sometimes replaced by

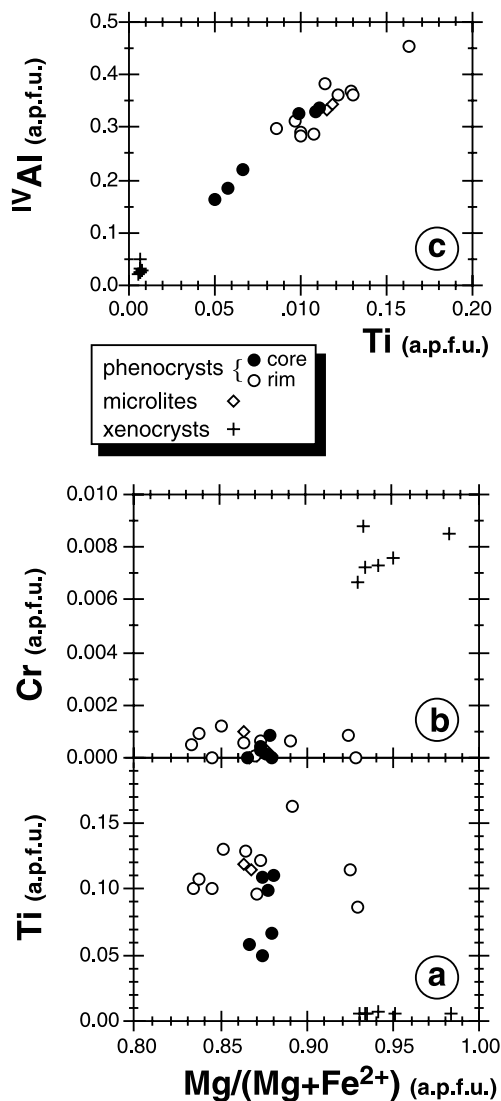


Fig. 3. Compositional variations of the clinopyroxene phenocrysts and xenocrysts from the Tchircotché monchiquites in the $\text{Mg}/(\text{Mg} + \text{Fe}^{2+})$ vs Ti (a), $\text{Mg}/(\text{Mg} + \text{Fe}^{2+})$ vs Cr (b) and Ti vs Al^{IV} (c) diagrams

calcite. Amphibole phenocrysts (up to 3.7 mm) are often zoned and frequently contain apatite inclusions. They are partially, and sometimes totally oxidized. Olivine phenocrysts (0.5–3.0 mm) occur only in some samples (<1% vol, *Ngounouno*, 1993) and are always completely altered and replaced by clinopyroxene, carbonates and chlorite. In spite of this alteration, the olivine can still be recognized by its typical habit. Minute lamellae (0.3×0.5 mm) of reddish brown biotite (<0.1 vol%) surround most of the titanomagnetite microphenocrysts in samples 2, 3 and 5. The analcitic microcrystalline matrix contains microlites of apatite and Fe–Ti oxides. Alkali feldspar and plagioclase microlites are absent in samples 6, 4, 8, 9, 7 and 1 but reach 15 vol% in samples 5, 3 and 2. The ocelli (<5 mm; 2 to 8 vol%) in the Tchircotché monchiquites consist either of carbonate–analcite or of carbonate–feldspar and may also contain small crystals of clinopyroxene, amphibole, Fe–Ti oxides, and chlorite spherulites.

Mineralogy

- *Olivine*. All the olivine phenocrysts are either completely pseudomorphosed or altered, there are no chemical data available.
- *Clinopyroxene*. The clinopyroxene phenocrysts (Fig. 3) have a diopsidic composition ($Wo_{48} En_{46} Fs_6$); they are Al-rich ($4.1 < Al_2O_3 < 10.1$ wt%) and Ti-rich ($1.8 < TiO_2 < 5.6$ wt%), the highest contents in these elements being found in the rims. The Al^{VI}/Al^{IV} ratio values show more variation in the cores (0.18–0.72) than in the rims (0.13–0.46); this corresponds to a low pressure of equilibration (*Wass*, 1979).
- *Amphibole*. According to the classification of *Leake et al.* (1997), the amphibole is a subsilicic kaersutite, ($5.5 < Si \text{ a.p.f.u.} < 5$; $52 < Mg\# < 70$). The phenocrysts are rich in Ti (up to 0.9 a.p.f.u.). Fluorine concentrations average 0.3 wt%. Equilibrium temperatures estimated after the Ti-amphibole geothermometer (*Otten*, 1984) are between 950 and 1050 °C ± 40 °C and correspond to low equilibration pressures (*Merrill and Wyllie*, 1975) as also attested, according to *Scott* (1980), by their low Al^{VI} (0.1 a.p.f.u.) and K (0.3 a.p.f.u.) contents.
- *Biotite*. The biotite ($52 < Mg\# < 76$) is Fe-rich ($Mg/Fe = 1.2$), Ti-rich (up to 10.2 wt%) and Al-rich. BaO contents vary from 0.1 to 4.0 wt%. Si and Al are not sufficient to fill the tetrahedral site ($Si + Al < 7.9$). Although the Fe_2O_3 content has not been measured directly, the presence of Fe^{3+} in tetrahedral site should be considered; this hypothesis is in agreement with high oxygen fugacity inferred from the abundance of titanomagnetite. Fluorine concentrations average 0.6 wt% but reach values up to 1.3 wt%. The high Ti, Al^{IV} and Ba contents, as well as the high $Mg\#$ of the biotite suggest crystallization at high temperature (≈ 1000 °C) and low pressure (≈ 1 kb) (estimation after *Hansen*, 1980).
- *Fe–Ti oxides*. Titanomagnetite ($47 < Usp\% < 50$) occurs as subhedral phenocrysts (3 to 5 mm). In samples 2 and 3, ilmenite lamellae are associated with titanomagnetite phenocrysts. Equilibrium temperatures of oxide pairs are between 820 °C and 880 °C (± 20 °C) and corresponding oxygen fugacities between 10^{-13} and 10^{-14} ($\pm 0.5 \times 10^{-14}$) atmospheres (calculations after *Spencer*

and *Lindsley*, 1981). However, these thermodynamic conditions are not considered to reflect those prevailing during their crystallization, but rather exsolution conditions.

- *Feldspars*. Sanidine (Or_{67-52}) occurs in the matrix as well as in carbonate ocelli. The values of $100 K/(Na + K)$ ratios (62.7–68.4) are lower than the average value of 72.7 for alkaline lamprophyres (*Rock*, 1987). The plagioclase is oligoclase (An_{16-29}) or albite (An_{0-5}) and is more calcic than the “typical plagioclase” (almost pure albite) of alkaline lamprophyres (*Rock*, 1987). Co-

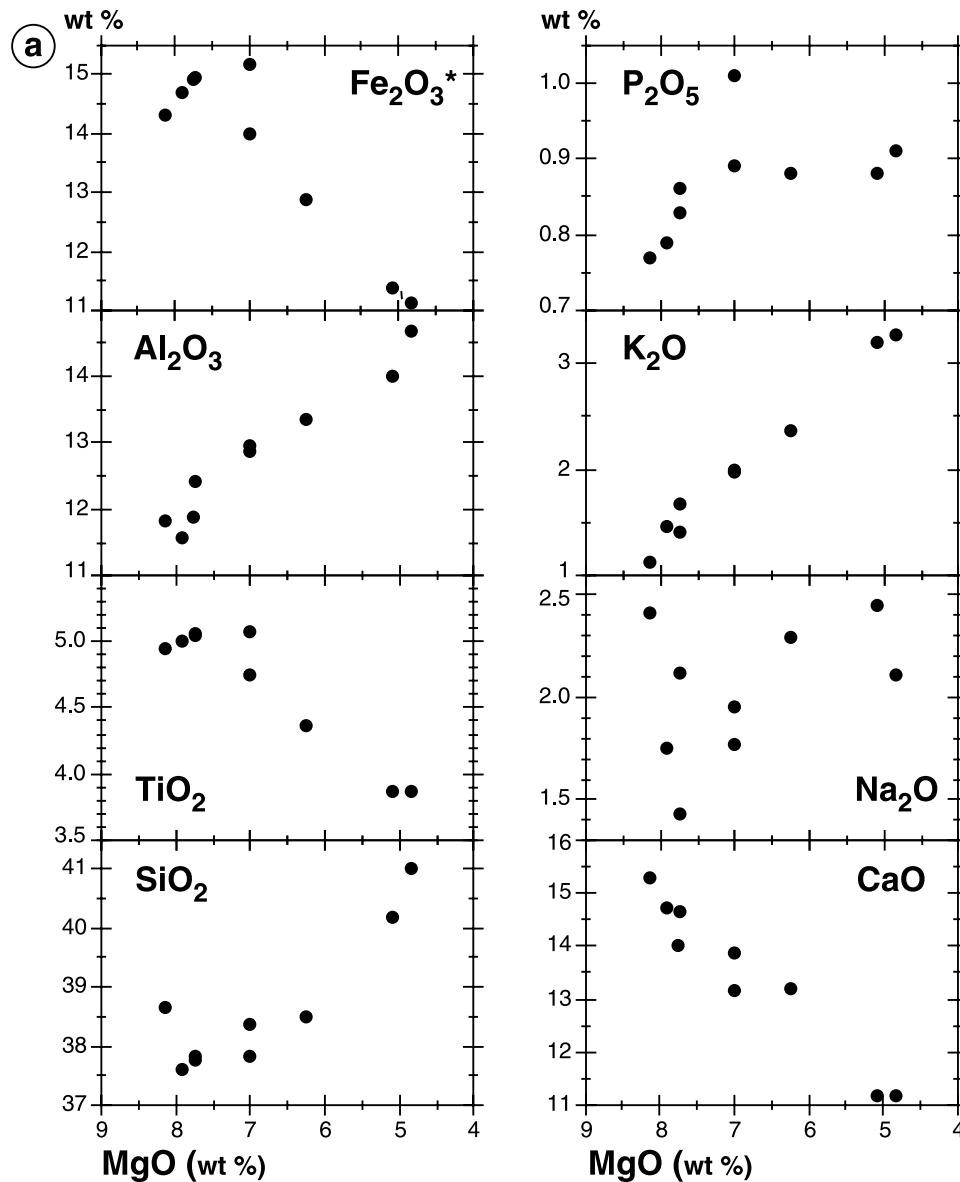


Fig. 4. Variation diagrams for Tchircotché monchiquites; **a** MgO vs. major elements (wt%) and **b** MgO vs. trace elements (ppm)

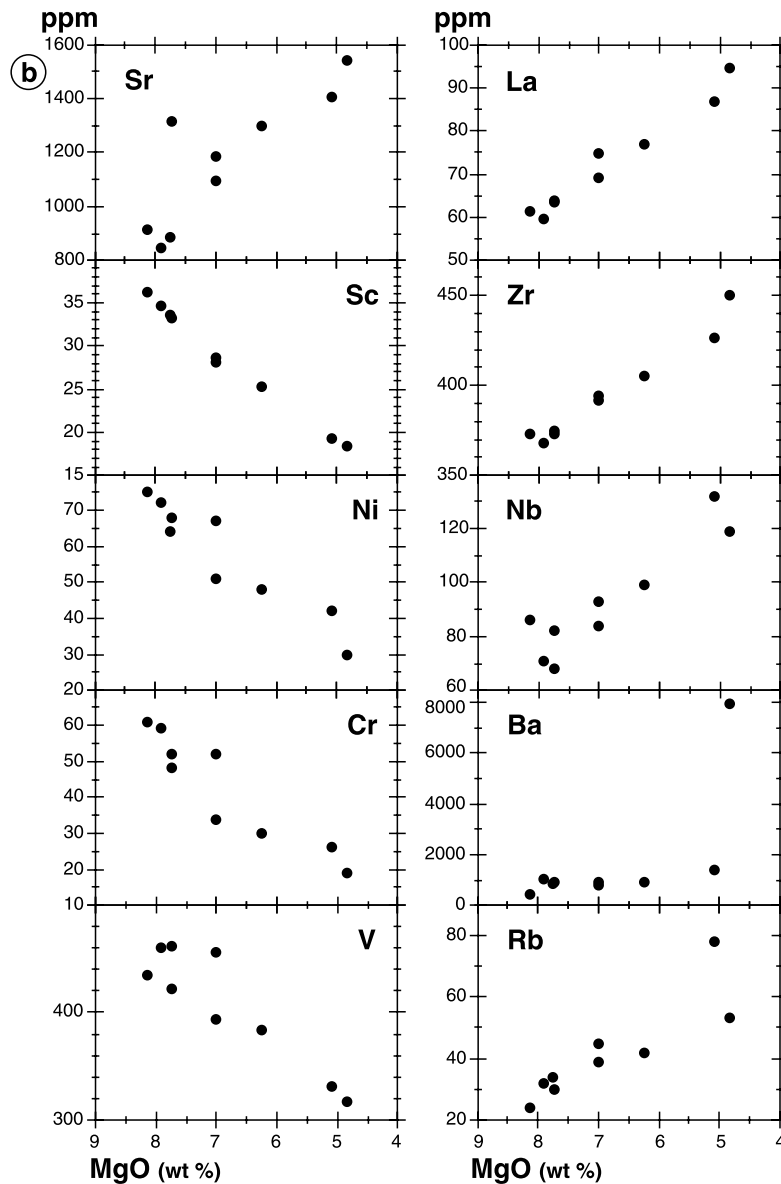


Fig. 4 (continued)

existing feldspar microlites (sanidine and oligoclase or albite) indicate low crystallization temperatures ($<550^{\circ}\text{C}$), below the solvus (Logfren, 1971; Mauger, 1988).

- *Apatite*. Apatite is the most abundant accessory mineral in the monchiquites (up to 5 vol%). The apatite phenocrysts have high fluorine contents (up to 3.6 wt% F) and significant amounts of rare earth elements ($\text{La}_2\text{O}_3 \approx 0.62$ wt% and $\text{Ce}_2\text{O}_3 \approx 0.31$ wt%). No compositional variation has been detected between core and rim, but there are substantial differences in REE, Sr, and Cl contents between crystals.

- *Analcite, calcite, and carbonate ocelli.* Analcite is generally present in the ocelli and as microlites. It contains numerous inclusions and is partly replaced by secondary calcite. In the ocelli, calcite crystals contain significant quantities of MgO (<1.6 wt%), FeO (<5 wt%), and MnO (<2 wt%).
- *Xenocrysts.* Rounded and fractured Cr-diopside xenocrysts are present. They have a fairly restricted compositional range (Fig. 3), with low Al, high Mg# (0.90–0.94) and Cr contents (up to 0.3 Cr₂O₃ wt%), high Al^{VI}/Al (expressed mainly as the Ca-Tschermak molecule), and moderate Na₂O contents (0.20 to 0.69 wt%) expressed as the jadeite molecule.

Geochemistry

Major and trace element compositions of samples of the Tchircotché monchiquite series are presented in Table 2. The monchiquites are typically silica-undersaturated ($37.6 < \text{SiO}_2 \text{ wt\%} < 41.0$; normative nepheline, \pm leucite and olivine). They have low magnesium contents [$4.8 < \text{MgO wt\%} < 8.1$; Mg# between 51 and 58 (Mg# = $100 \text{ Mg} / (\text{Mg} + \text{Fe}^{2+})$ with Fe^{2+} calculated assuming $\text{Fe}^{2+} / \text{Fe}^{3+} = 0.20$)],

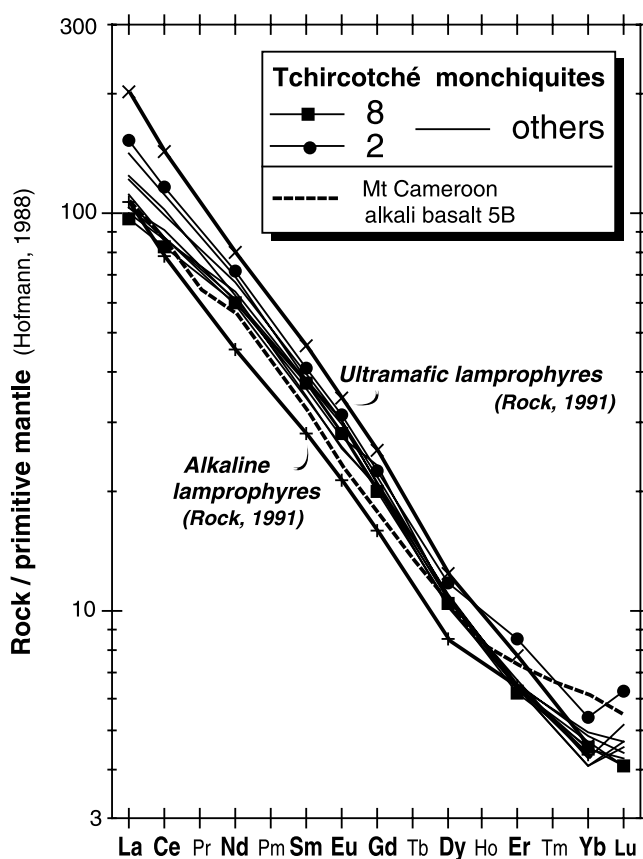


Fig. 5. Primitive mantle (Hofmann, 1988) normalized rare-earth element diagram for Tchircotché lamprophyres

and are rich in alkalis ($3.1 < (\text{Na}_2\text{O} + \text{K}_2\text{O}) \text{ wt}\% < 5.7$), TiO_2 (3.9–5.1 wt%) and P_2O_5 (0.8–1.0 wt%).

Broadly, there are good linear correlations between MgO and the major oxides, except Na_2O and P_2O_5 (Fig. 4a). The SiO_2 , Al_2O_3 and K_2O contents increase with increasing differentiation of the monchiquites (expressed as a decrease in MgO contents) whereas CaO contents decrease. The TiO_2 , Fe_2O_3 and P_2O_5 first increase slightly, then decrease (or remain constant: P_2O_5) when MgO is lower than 7 wt%. The scatter of the Na_2O data could be due to variations of the depth of melting and/or of the degree of melting. High water contents in Tchircotché lamprophyres are attested by the abundance of kaersutite (and biotite) phenocrysts. Such high water contents characterize not only the magma source but also the late stage of evolution when groundmass analcite crystallized. At this late stage, the H_2O content could have been high enough to allow a separation of a fluid phase from the melt.

Concentrations of most compatible trace elements (Sc, Ni, Cr, V) decrease with increasing differentiation (Fig. 4b) whereas those of incompatible elements (Sr, Rb,

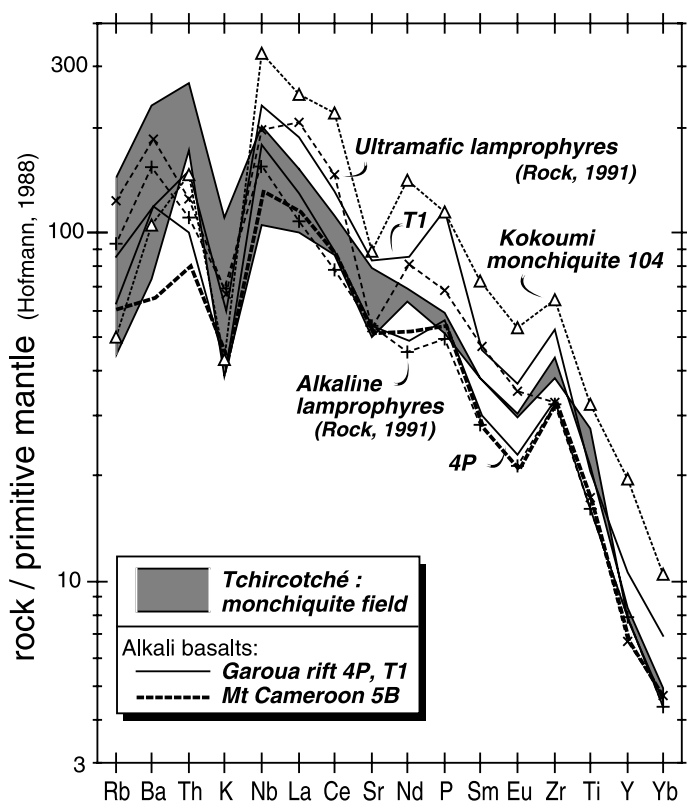


Fig. 6. Primitive mantle (Hofmann, 1988) normalized multi-element diagrams for Tchircotché lamprophyres. The average of alkaline and ultramafic lamprophyres (Rock, 1991), the Kokoumi monchiquite (104, Ngounouno et al., 2001) and alkali basalts from the Garoua rift (4P and T1, Ngounouno et al., 1997a) and Mt Cameroon (5B, Déruelle et al., unpubl.) are also plotted for comparison

Table 3. Rb–Sr and Sm–Nd isotopic data of Tchircotché monchiquites

Sample	Rb (ppm)	Sr (ppm)	$^{87}\text{Rb}/^{86}\text{Sr}$	$^{87}\text{Sr}/^{86}\text{Sr}$	2σ	$(^{87}\text{Sr}/^{86}\text{Sr})_{37\text{Ma}}$	Sm (ppm)	Nd (ppm)	$^{147}\text{Sm}/^{144}\text{Nd}$	$^{143}\text{Nd}/^{144}\text{Nd}$	2σ	$\varepsilon_{\text{Nd}(37\text{Ma})}$
6	29.3	1314	0.0645	0.703689	0.000008	0.70366	14.0	71.5	0.1184	0.512745	0.000007	2.46
2	50.0	1542	0.0995	0.703926	0.000007	0.70387	15.8	85.2	0.1121	0.512753	0.000009	2.65
standard				0.710263	0.000009					0.511964	0.000009	
				0.710265	0.000010							

Ba, La, Nb, Zr) increase. The most differentiated rock (sample 2) displays a very high Ba content (7900 ppm). The lamprophyres have a very homogeneous rare-earth element distribution, with light REE enriched parallel patterns in a primitive mantle normalized diagram (Fig. 5). Nevertheless, there is a larger variation range for light REE ($60 < \text{La ppm} < 95$) compared to heavy REE ($1.7 < \text{Yb ppm} < 2.2$) with $21.4 < (\text{La/Yb})_N < 30.7$ and $2.6 < (\text{La/Sm})_N < 3.8$. The most differentiated sample (2) has the highest REEs. The Tchircotché monchiquites plot in the narrow field limited by the patterns of average alkaline and ultramafic lamprophyres (Rock, 1991). They have high $(\text{Ce/Yb})_N$ ratios (mean value $\approx 21.0 \pm 2.1$) resulting in steeper patterns than those for basalts from the Kapsiki plateau (14.3 ± 2.5 , Ngounouno et al., 2000) and Mt Cameroon (15.2 ± 2.5 , Déruelle et al., unpublished data).

In a primitive mantle-normalized spider diagram (Fig. 6), the range between the lowest (L) and the highest (H) values is quite large for the most incompatible elements, from Rb to Sr with $\text{Rb}_L/\text{Rb}_H \approx 3.3$, and, on the contrary, very narrow for the less incompatible elements, from Nd to Yb ($\text{Nd}_L/\text{Nd}_H \approx 1.1$). The contents of Rb, Ba, Th and K are higher than in other lamprophyres from the Garoua rift (Ngounouno et al., 2003). All samples have a typical K-depletion. The monchiquite patterns are almost parallel to those of the least differentiated basalts from the Cameroon Line and the Garoua rift (Fig. 6). Generally, the monchiquites have similar contents or are enriched in most incompatible elements in comparison with basalts.

The Tchircotché monchiquites have initial (recalculated for an age of 37 Ma) $^{87}\text{Sr}/^{86}\text{Sr}$ and ε_{Nd} isotopic values of 0.70366–0.70387 and +2.5–2.7 respectively (Table 3). These isotopic compositions are roughly similar to those obtained for basalts from the continental and oceanic segments of the Cameroon Line (range of values: $^{87}\text{Sr}/^{86}\text{Sr}$: 0.7030–0.7038; ε_{Nd} : +2 to +4; Halliday et al., 1988; Ngounouno et al., 2000, 2003; Demaiffe et al., unpublished results) and Adamawa Plateau (Nono et al., 1994; Marzoli et al., 2000).

Age

One monchiquite sample has been dated by whole-rock K–Ar at 37.5 ± 2.3 Ma. Other volcanic and plutonic rocks from the Garoua rift, East of Tchircotché, have also been dated between 34.8 ± 0.8 and 39.7 ± 0.9 Ma (Ngounouno et al., 2003).

Discussion

Differentiation by fractional crystallization

The major element compositions (Table 2) allow to discriminate the Mg-rich samples (6, 8, 9, 4, 1 and 7, with $\text{MgO} > 7.0$ wt%) with low loss-on-ignition (LOI: 2.0 to 3.9 wt%), CO_2 (0.21 to 0.82 wt%) and K_2O (< 2.0 wt%) contents from those with $\text{MgO} < 7.0$ wt% (samples 3, 5 and 2) which have significantly higher LOI (up to 6.4 wt%), CO_2 (up to 2.6 wt%) and K_2O (> 2.3 wt%) contents. Despite these differences in major elements, the incompatible elements (e.g. Rb, Sr, Th, Nb, LREE) increase regularly with decreasing MgO, while the compatible element concentrations (e.g. Ni, Cr and Sc) decrease rapidly with increasing incompatible element concentrations (Fig. 4a, b), leading to the suggestion that

all the samples form a single suite evolving from Mg-rich samples to alkali-rich differentiates, and that fractional crystallization is the process that governs the differentiation of the series. It appears that a first step of fractionation involving olivine is necessary. Modelling of the second step by means of mass-balance fractionation for major elements gave results which are consistent with the distribution of the mineralogical phases present as phenocrysts in the rocks. For example, the slightly differentiated sample 7 can be derived from the primitive monchiquite sample 6 by fractionation of pyroxene (8.3 wt%) and amphibole (0.4 wt%) ($\Sigma r^2 < 2.0$). The most differentiated sample 2 can be derived from sample 7 by fractionation of pyroxene (9.6 wt%), amphibole (18.1 wt%), magnetite (6.5 wt%) and apatite (0.2 wt%) ($\Sigma r^2 < 1.9$). However, the decrease of the CaO content with increasing differentiation (Fig. 4a) and the slightly concave-upwards middle REE patterns (Fig. 5) may be attributed to crystal fractionation of amphibole, which is an abundant (up to 15% vol) phenocryst in the monchiquites. Zircon, apatite and sphene should be absent in the residue of the monchiquite suite as suggested by the incompatible behavior of elements such as Zr, light REE, and P (Fig. 4, 6).

Magma source

Any attempt to outline the source characteristics of the Tchircotché magmas must account for the following observations:

- (i) the monchiquites are characterized by low contents of SiO₂, and very low concentrations of compatible element (Sc, Cr and Ni) (Table 2 and Fig. 4).
- (ii) all the monchiquites have very high concentrations of incompatible elements and are strongly enriched in light REE (e.g., $97 < La_N < 157$) relative to heavy REE (Fig. 5) which argues against an origin by partial-melting from an upper-mantle source.
- (iii) on normalized multi-element plots (Fig. 6), most of the rocks are depleted in K and Rb and all rocks are rich in Ba, Sr, Ti, Nb and P.
- (iv) the magmas are derived from a source with time integrated Rb/Sr and Sm/Nd ratios that are lower than bulk-Earth.

Nature of the source

In general, alkaline lamprophyre magmas are believed to originate from the upper mantle (Rock, 1991; Delor and Rock, 1991; Ulrych et al., 1993). Accordingly, high concentrations of Cr, Ni and high Mg# would be expected in such magmas, but the Tchircotché monchiquites are unusual (when compared to other monchiquites worldwide) in that they contain low Cr (<70 ppm) and Ni (<76 ppm) and have rather low Mg# (51–58). It is of course difficult to assess whether monchiquites correspond to magmas already differentiated by early olivine ± clinopyroxene fractionation or to primary (= undifferentiated) magmas resulting from low degrees of partial melting of a carbonated lherzolite, as proposed for ultramafic lamprophyres (Dalton and Presnall, 1998).

The Cr-diopside xenocrysts of the Tchircotché monchiquites are similar in composition to those found in other alkali basalt (*Stosch and Seck, 1980*). Their restricted compositional range (Fig. 3) and the fact that their chemical and isotopic composition is distinct from that of their host magma has led to the interpretation that these clinopyroxenes are xenocrystic fragments derived from lithospheric peridotites. The Cr-rich xenocrysts of Tchircotché are often fractured, they display sieved areas and have rounded shapes that could result from reaction with a hot magma after assimilation. Pressure and temperature estimates for these Cr-diopside xenocrysts suggest that they equilibrated at 1200–1250 °C (*Thompson, 1974*), between 10 and 15 kb (*Aoki, 1971*) corresponding to a depth of 35–40 km, that is to say within the spinel lherzolite field, just below the regional crust–mantle boundary (20–30 km; *Poudjom Djomani et al., 1997*).

The Ba content of the most evolved monchiquite (sample 2) is extremely high (7900 ppm) when compared to those of other samples. This high content cannot be explained by crustal contamination because of the high Sr content (1542 ppm) and the low initial $^{87}\text{Sr}/^{86}\text{Sr}$ value (0.70368 ± 10) of this sample, and because of the absence of negative Nb anomaly (Fig. 6).

The abundances of some diagnostic trace and major elements in monchiquite liquids can be used to precise the mineralogical composition of their mantle source. As previously stated, the depletion in K and Rb on the mantle normalized trace element patterns of monchiquites (Fig. 6) requires the presence of a potassic mineral in the residue of their mantle source. Phlogopite has mineral/melt partition coefficients for Rb and K higher than 1 in basaltic systems (*Foley et al., 1996*). In the presence of fluorine, phlogopite is stable up to high pressures (6–7 GPa; *Foley, 1989*; *Sudo and Tatsumi, 1990*) where it decomposes to form numerous phases including potassic amphibole. The negative K and Rb anomalies in the normalized multi-element patterns of monchiquites suggest that the residual phase was phlogopite rather than amphibole. The stability of phlogopite and the low solubility of K in the melt are thought to be enhanced by high $\text{CO}_2/(\text{CO}_2 + \text{H}_2\text{O})$ and $\text{F}/\text{H}_2\text{O}$ conditions (*Edgar and Vukadinovic, 1992*; *Foley, 1989*). Currently, we have not been able to determine conclusively if amphibole was present in the source. The strong depletion of heavy REE (Fig. 5) in the monchiquites could reflect either the occurrence of garnet as a residual phase during partial melting in the mantle or the high pressure garnet fractionation. As an alternative hypothesis, it has been suggested (i.e. *Chauvel et al., 1992*) that K negative anomaly is a characteristic of the source of the alkali basalts with HIMU Pb isotope signatures, such as the alkali basalts of the Cameroon Line (*Halliday et al., 1990*).

Experiments (*Dalton and Presnall, 1998*) and isotopic data (*Simonetti and Bell, 1995*) have shown that very low degrees of partial melting of carbonated, hydrated peridotites may produce ne-normative, volatile-bearing melts. The Tchircotché lamprophyre magmas are silica-undersaturated, they have steep REE patterns (Fig. 5), high incompatible element contents and high (La/Yb)_N values (21.4–30.7) when compared to the basalts of the Cameroon Line ($12 < \text{LaN}/\text{YbN} < 22$; *Déruelle* unpublished data) (Fig. 6). Therefore, the degree of partial melting should be lower for the monchiquite magma than for the alkali basalt magma. The large range of highly incompatible element contents (from Rb to Sr in Fig. 6) and the narrow range of the less incompatible elements (from Nd to Yb in Fig. 6) for the different monchiquites

suggest either variations in the degree of partial melting of a common mantle source or discrete melting events of variously metasomatized mantle sources.

Mantle metasomatism

To generate partial melts with high concentrations of incompatible elements (light REE, Ba, Sr), the mantle source must have been previously enriched in these elements (e.g. *Delor and Rock, 1991; Wu and Berg, 1992; Ulrych et al., 1993; Hoch, 1999*). Major element, trace element and Sr–Nd–Pb isotopic compositions of the ultramafic xenoliths and megacrysts from the Cameroon Line (*Lee et al., 1996*) provide evidence for metasomatism of the uppermost lithospheric mantle by enriched fluids during the Mesozoic. High incompatible element contents (Table 2) and the occurrence of volatile- and halogen-rich minerals (amphibole, biotite, carbonate) in the Tchircotché monchiquites, as well as experiments on CO₂- and H₂O-rich peridotites (*Dalton and Presnall, 1998* and references herein) suggest that these monchiquites originated from an infra-lithospheric metasomatized peridotite. The existence of these volatile-rich phases in the upper mantle should be connected with metasomatizing fluids fixed at depths near the high-pressure limit of stability of the above minerals (e.g., *Dautria et al., 1992; Hauri et al., 1993; Rudnick et al., 1993; McDonough and Rudnick, 1998*). These conditions are typical at the base of areas subjected to continental lithosphere extension and this may account for the occurrence of alkaline lamprophyres in a few well-defined tectonic environments such as continental rifts.

Metasomatized peridotites are considered to be representative of enriched sub-continental lithosphere. Melts forming K-rich amphibole are now considered to be a common metasomatic agent of the upper mantle, forming a network of thin dykes lacing mantle peridotite beneath zones of recent volcanism (e.g., *Witt-Eickschen et al., 1998; Lee et al., 1996; Déruelle et al., 2001*). The common occurrence and the high modal proportions of amphibole in xenoliths from the upper mantle along the Cameroon Line suggest that the lithospheric mantle has been metasomatized. We regard this as further evidence of a K-rich precursor metasomatic fluid in the infra-lithospheric mantle beneath the Cameroon Line.

Globular structures, such as ocelli and segregations of irregular shape, are known in lamprophyres worldwide. *Rock (1991)* has defined three types of ocelli in lamprophyres on the basis of their mineralogical association: i) carbonate–analcite is commonly found in alkaline and ultramafic lamprophyres, ii) carbonate–feldspar, approaching syenitic composition, is found mainly in alkaline lamprophyres and very rarely in ultramafic lamprophyres, and iii) carbonate–chlorite–quartz is usually found in all lamprophyre groups and in ocelli in alkali basalts. The ocelli in the Tchircotché monchiquites consist either of carbonate–analcite or of carbonate–feldspar; they must represent the last alkali- and volatile-rich residual fluids.

The Tchircotché monchiquites and the Cameroon Line basalts

The monchiquites of the Tchircotché area have trace element and REE patterns similar to those of Mt Cameroon and Garoua rift basalts (Fig. 6). The initial

isotopic composition of the monchiquites ($^{87}\text{Sr}/^{86}\text{Sr} = 0.70366\text{--}0.73687$; ε_{Nd} : +2.5 to +2.7) are quite similar to those of basalts from the continental and oceanic segments of the Cameroon Line (range of values: $^{87}\text{Sr}/^{86}\text{Sr} = 0.7030\text{--}0.7038$; $\varepsilon_{\text{Nd}} = +2$ to +4; *Halliday et al.*, 1988; *Ngounouno et al.*, 2000, 2003; *DemaiFFE et al.*, unpublished results) and from the Adamawa Plateau (*Nono et al.*, 1994; *Marzoli et al.*, 2000) precluding involvement of crustal materials in their genesis. The geochemical and isotopic similarities between the Tchircotché monchiquites and the least differentiated basalts of the Cameroon Line are a strong argument suggesting magma sources with similar compositions for both lamprophyres and basalts. Despite the apparent lack of high-pressure xenocrysts along the Cameroon Line which led *Lee et al.* (1996) to propose a shallow lithospheric source for the magmas, it has already been demonstrated that the mantle source for basalts of the Cameroon Line is infra-lithospheric (*Déruelle et al.*, 1991). It is a fact that the nature and evolution of the lithosphere is very different for the young (<140 Ma) oceanic segment of the Cameroon Line and for the old (>500 Ma) continental segment of this Line. The reservoir of HIMU-type, according to the Pb isotopic data (*Halliday et al.*, 1990; *Lee et al.*, 1994; *Ballentine et al.*, 1997), should have provided individual batches of primary magma that mixed with both enriched and depleted upper mantle components before they differentiated along the same general trend, all along the Line.

Conclusions

The petrogenesis of the Tchircotché monchiquites can be tentatively explained as follows. The primitive parental magma results from low degree of partial melting of an infra-lithospheric metasomatized garnet-bearing peridotite mantle. This mantle source has geochemical characteristics comparable to the source which generated alkaline basaltic magmas all along the Cameroon Line. The monchiquite parental magma rose through the lithosphere and ponded in its upper part (35–40 km) where Cr-diopside xenocrysts have been incorporated. Fractional crystallization of olivine + clinopyroxene + hornblende + Fe–Ti oxides + apatite gave rise to the distinct magma batches from which the monchiquite dykes erupted during Eocene times in an extensional tectonic setting. Late crystallization of calcite (development of ocelli) and analcite as well as the late transformation of most phenocrysts (olivine, clinopyroxene replaced by calcite, kaersutite replaced by Fe–Ti oxides) attest to the important role played by CO₂-, H₂O- and F-rich fluids during the ultimate stage of crystallization, at upper levels in the continental crust.

Acknowledgements

The French Ministère de la Coopération is acknowledged for providing grants to *I.N.* for stays in France in the Laboratoire de Magmatologie et de Géochimie Inorganique et Expérimentale, Université Pierre et Marie Curie, Paris, and for financially supporting the research work. This work is part of a Thèse de l'Université Pierre et Marie Curie (Paris VI) by *I.N.* Fieldwork (*I.N.* and *B.D.*) was substantially supported by the Faculty of Science of the University of Yaoundé (Dean, Prof. *G. Valet*). The isotopic measurements at the Université Libre de Bruxelles were financially supported by the Ministère des Affaires Economiques

(projet SGB/NAT 91–98). The constructive comments of *G. Caprarelli*, *J. Foden* and *M. Elburg* are greatly appreciated.

References

- Aoki K* (1971) Petrology of mafic inclusions from Itinomegata, Japan. *Contrib Mineral Petrol* 30: 314–330
- Ashwal LD, Demaiffe D, Torsvik TH* (2002) Petrogenesis of Neoproterozoic granitoids and related rocks from the Seychelles: the case for an Andean-type arc origin. *J Petrol* 43: 45–83
- Ballentine CJ, Lee D-C, Halliday AN* (1997) Hafnium isotopic studies of the Cameroon line and new HIMU paradoxes. *Chem Geol* 139: 111–124
- Benkhelil J* (1988) Structure et évolution géodynamique du bassin intracontinental de la Bénoué (Nigéria). *Bull Centres Rech Explor-Prod Elf-Aquitaine* 17: 29–128
- Bonhomme M, Thuizat R, Pinault Y, Clauer N, Wendling A, Winkler R* (1975) Méthode de datation potassium-argon. Appareillage et technique. *Notes Techn Inst Géol Univ Louis Pasteur Strasbourg* 3: 1–53
- Carignan J, Hild P, Mévelle G, Morel J, Yeghicheyan D* (2001) Routine analyses of trace elements in geological samples using flow injection and low pressure on-line liquid chromatography coupled to ICP-MS: a study of geochemical reference materials BR, DR-N, UB-N, AN-G and GH. *Geostandards Newslett* 25: 187–198
- Chauvel C, Hofmann AW, Vidal P* (1992) HIMU-EM: the French Polynesian connection. *Earth Planet Sci Lett* 110: 99–119
- Clarke DB, Muecke GK, Pe-Piper G* (1983) The lamprophyres of Ubekendt Ejland, West Greenland: products of renewed partial melting or extreme differentiation. *Contrib Mineral Petrol* 83: 117–127
- Cox A, Dalrymple GB* (1967) Statistical analysis of geomagnetic reversal data and the precision of potassium-argon dating. *J Geophys Res* 72: 2603–2614
- Dalton JA, Presnall DC* (1998) Carbonatitic melts along the solidus of model lherzolite in the system CaO–MgO–Al₂O₃–SiO₂–CO₂ from 3 to 7 GPa. *Contrib Mineral Petrol* 131: 123–135
- Dautria JM, Dupuy C, Takherist D, Dostal J* (1992) Carbonate metasomatism in the lithospheric mantle: peridotitic xenoliths from a melilititic district of the Sahara Basin. *Contrib Mineral Petrol* 111: 37–52
- Delor CP, Rock NMS* (1991) Alkaline-ultramafic lamprophyre dikes from the Vestfold Hills, Princess Elizabeth Land (East Antarctica): primitive magmas of deep mantle origin. *Antarctic Sci* 3: 419–432
- Déruelle B, Moreau C, Nkoumbou C, Kambou R, Lissom J, Njongfang E, Ghogomu RT, Nono A* (1991) The Cameroon Line: a review. In: *Kampunzu AB, Lubala RT* (eds) *Magmatism in extensional structural settings. The Phanerozoic African Plate*. Springer, Berlin Heidelberg New York Tokyo, pp 274–327
- Déruelle B, Ngounouno I, Bardintzeff JM* (2001) Wehrlites et pyroxénites en nodules dans les basaltes du Mt Cameroun : évidence d'un métasomatisme mantellique. *J Soc Geosci Africa* 1: 90–91
- Déruelle B, Ngounouno I, Nkoumbou C* (1998) Mt Cameroon, Mt Etinde, and Bioko Island volcanoes of the “Cameroon hot Line”. Evolution of Ocean Island Volcanoes, Penrose Conf Ser, Galapagos Islands 4–12 June, Abstr vol, p 28
- Droop GTR* (1987) A general equation for estimating Fe³⁺ concentrations in ferromagnesian silicates and oxides from microprobe analyses, using stoichiometric criteria. *Mineral Mag* 51: 431–435

- Edgar AD, Vukadinovic D (1992) Implications of experimental petrology to the evolution of ultrapotassic rocks. *Lithos* 28: 205–220
- Foley SF (1989) The genesis of lamproitic magmas in a reduced, fluorine-rich mantle. In: Jaques AL, Ferguson J, Green DH (eds) *Kimberlites and related rocks 1*. Blackwell, Melbourne, pp 616–632
- Foley SF, Jackson SE, Fryer BJ, Greenough JD, Jenner GA (1996) Trace element partition coefficients for clinopyroxene and phlogopite in an alkaline lamprophyre from Newfoundland by LAM-ICP-MS. *Geochim Cosmochim Acta* 60: 629–638
- Guiraud M (1993) Late Jurassic-Early Cretaceous rifting and Late Cretaceous transpressional inversion in the Upper Benue basin (NE Nigeria). *Bull Centres Rech Explor-Prod Elf-Aquitaine* 17: 371–383
- Guiraud R, Bosworth W (1997) Senonian basin inversion and rejuvenation of rifting in Africa and Arabia: synthesis and implications to plate-scale tectonics. *Tectonophysics* 282: 39–82
- Halliday AN, Davidson JP, Holden P, DeWolf CP, Lee DC, Fitton JG (1990) Trace-element fractionation in plume and origin of HIMU mantle beneath the Cameroon line. *Nature* 347: 523–528
- Halliday AN, Dickin AP, Fallick AE, Fitton JG (1988) Mantle dynamics: a Nd, Sr, Pb and O isotopic study of the Cameroon line volcanic chain. *J Petrol* 29: 181–211
- Hansen K (1980) Lamprophyres and carbonatitic lamprophyres related to rifting in the Labrador Sea. *Lithos* 13: 145–153
- Hauri EH, Shimizu N, Dieu JJ, Hart SR (1993) Evidence for hotspot-related carbonatite metasomatism in the oceanic upper mantle. *Nature* 365: 221–227
- Hoch M (1999) Geochemistry and petrology of ultramafic lamprophyres from Schirmacher Oasis, East Antarctica. *Mineral Petrol* 65: 51–67
- Hofmann A (1988) Chemical differentiation of the Earth: the relationship between mantle, continental crust, and oceanic crust. *Earth Planet Sci Lett* 90: 297–314
- Jelinek E, Soucek J, Tvrdy J, Ulrych J (1989) Geochemistry and petrology of alkaline dike rocks of the Roztoky volcanic centre, Ceske Stredohori Mountains, CSSR. *Chemie der Erde* 49: 201–217
- Kampunzu AB, Popoff M (1991) Distribution of the main Phanerozoic African rifts and associated magmatism: introductory notes. In: *Kampunzu AB, Lubala RT (eds) Magmatism in extensional structural settings. The Phanerozoic African Plate*. Springer, Berlin Heidelberg New York Tokyo, pp 2–10
- Leake BE (chairman) and 20 co-authors (1997) Nomenclature of amphiboles: report of the Subcommittee on amphiboles of the International Mineralogical Association Commission on new minerals and mineral names. *Mineral Mag* 61: 295–321
- Lee D-C, Halliday AN, Davies GR, Essene EJ, Fitton GJ, Temdjim R (1996) Melt enrichment of shallow depleted mantle: a detailed petrological, trace element and isotopic study of mantle-derived xenoliths and megacrysts from the Cameroon Line. *J Petrol* 37: 415–441
- Logfren GE (1971) Spherulitic textures in glassy and crystalline rocks. *J Geophys Res* 76: 5635–5648
- Marzoli A, Piccirillo EM, Renne PR, Bellieni G, Lacumin M, Nyobe JB, Tongwa AT (2000) The Cameroon Volcanic Line revisited: petrogenesis of continental basaltic magmas from lithospheric and asthenospheric mantle sources. *J Petrol* 41: 87–109
- Marzoli A, Renne PR, Piccirillo EM, Francesca C, Bellieni G, Melfi AJ, Nyobe JB, N'ni J (1999) Silicic magmas from the continental Cameroon Volcanic Line (Oku, Bambouto and Ngaoundere): ^{40}Ar – ^{39}Ar dates, petrology, Sr–Nd–O isotopes and their petrogenetic significance. *Contrib Mineral Petrol* 135: 133–150

- Mauger RL* (1988) Ocelli: transient disequilibrium features in a lower Carboniferous minette near Concord, North California. *Can Mineral* 26: 117–131
- Maury RC, Defant MJ, Joron JL* (1992) Metasomatism of the sub-arc mantle inferred from trace elements in Philippines xenoliths. *Nature* 360: 661–663
- McDonough WF, Rudnick RL* (1998) Mineralogy and composition of the upper mantle. In: *Hemly RJ* (ed) Ultrahigh-pressure mineralogy: physics and chemistry of the Earth's deep interior. *Min Soc Am Rev Mineral* 37: 139–175
- McKenzie DP* (1989) Some remarks on the movement of small melt fractions in the mantle. *Earth Planet Sci Lett* 95: 53–72
- Merrill RB, Wyllie PJ* (1975) Kaersutite and kaersutite-eclogite from Hakanni, New Zealand. Water excess and water deficient melting to 30 kbars. *Bull Geol Soc Am* 86: 555–570
- Meyers JB, Rosendahl BR, Harrison CGA, Ding Z-A* (1998) Deep-imaging seismic and gravity results from the offshore Cameroon Volcanic Line, speculation of African hotlines. *Tectonophysics* 284: 31–63
- Mitchell RH, Platt RG, Ladéroue DG* (1991) Petrology of alkaline lamprophyres from the Coldwell alkaline complex, northwestern Ontario. *Can J Earth Sci* 28: 1653–1663
- Montigny R, Le Mer O, Thuizat R, Whitechurch H* (1988) K–Ar and ^{40}Ar – ^{39}Ar study of metamorphic rocks associated with the Oman ophiolite: tectonic implications. *Tectonophysics* 151: 341–362
- Moreau C, Regnault JM, Déruelle B, Robineau B* (1987) A new tectonic model for the Cameroon Line, Central Africa. *Tectonophysics* 139: 317–334
- Morimoto N* (1989) Nomenclature of pyroxenes. *Can Mineral* 27: 143–156
- Ngounouno I* (1993) Pétrologie du magmatisme cénozoïque de la vallée de la Bénoué et du plateau Kapsiki (nord du Cameroun). Thesis, Univ Pierre et Marie Curie Paris, 280 pp
- Ngounouno I, Déruelle B, Demaiffe D* (2000) Petrology of the bimodal Cenozoic volcanism of the Kapsiki Plateau (northernmost Cameroon, Central Africa). *J Volcanol Geotherm Res* 102: 21–44
- Ngounouno I, Déruelle B, Demaiffe D, Montigny R* (2003) Petrology of the Cenozoic volcanism in the Upper Benue valley, northern Cameroon (Central Africa). *Contrib Mineral Petrol* 145: 87–106
- Ngounouno I, Moreau C, Déruelle B, Demaiffe D, Montigny R* (2001) Pétrologie du complexe alcalin sous-saturé de Kokoumi (Cameroun). *Bull Soc Géol France* 172: 451–460
- Ngounouno I, Nkoumbou C, Loulé JP* (1997b) Relations entre l'évolution tectono-sédimentaire et le magmatisme du fossé de Garoua (Nord du Cameroun). *Afr Geosci Rev* 4: 451–460
- Ngounouno I, Déruelle B, Demaiffe D, Montigny R* (1997a) Données nouvelles sur le volcanisme cénozoïque du fossé de Garoua (Nord du Cameroun). *CR Acad Sci Paris, Sér IIa* 325: 87–94
- Nono A, Déruelle B, Demaiffe D, Kambou R* (1994) Tchabal Nganha volcano in Adamawa (Cameroon): petrology of a continental alkaline lava series. *J Volcanol Geotherm Res* 60: 147–178
- Otten MT* (1984) The origin of brown hornblende in the Artfjallet gabbro and dolerites. *Contrib Mineral Petrol* 86: 189–199
- Pouchou JL, Pichoir F* (1991) Quantitative analysis of homogeneous or stratified micro-volumes applying the model "PAP". In: *Heinrich KFJ, Newbury DE* (eds) Electron probe quantification. Plenum Press, New York, pp 31–75
- Poudjom Djomani YH, Diament M, Wilson M* (1997) Lithospheric structure across the Adamawa plateau (Cameroon) from gravity studies. *Tectonophysics* 273: 317–327

- Rock NMS* (1987) The nature and origin of lamprophyres: an overview. In: *Fitton JG, Upton BCG* (eds) Alkaline igneous rocks. Blackwell, Edinburgh, pp 191–226
- Rock NMS* (1991) Lamprophyres. Blackie and Sons Ltd, Glasgow, 285 p
- Rudnick RL, McDonough WF, Chappell BW* (1993) Carbonatite metasomatism in the northern Tanzanian mantle: petrographic and geochemical characteristics. *Earth Planet Sci Lett* 114: 463–475
- Scott PW* (1980) Zoned pyroxenes and amphiboles from camptonites near Gran, Oslo region, Norway. *Mineral Mag* 43: 913–917
- Simonetti A, Bell K* (1995) Nd, Pb and Sr isotopic data from the Mount Elgon volcano, Eastern Uganda–western Kenya: implications for the origin and evolution of nepheline lavas. *Lithos* 36: 141–153
- Spencer KJ, Lindsley DH* (1981) A solution model for coexisting iron-titanium oxides. *Am Mineral* 66: 1189–1201
- Steiger RH, Jäger E* (1977) Subcommittee on geochronology: convention on the use of decay constants in geo- and cosmochronology. *Earth Planet Sci Lett* 36: 359–362
- Stormer C Jr* (1983) The effects of recalculation on estimates of temperature and oxygen fugacity from analyses of multicomponent iron-titanium oxides. *Am Mineral* 68: 586–594
- Stosch HG, Seck HA* (1980) Geochemistry and mineralogy of the two spinel peridotite suites from Dreiser Weiher, West Germany. *Geochim Cosmochim Acta* 44: 457–470
- Sudo A, Tatsumi Y* (1990) Phlogopite and K-amphibole in the upper mantle: implication for magma genesis in subduction zones. *Geophys Res Lett* 17: 29–32
- Thompson RN* (1974) Some high-pressure pyroxenes. *Mineral Mag* 39: 768–787
- Ulrych J, Pivec E, Zak K, Bendl J, Bosak P* (1993) Alkaline and ultramafic carbonate lamprophyres in central Bohemian Carboniferous basins, Czech Republic. *Mineral Petrol* 48: 65–81
- Wass SY* (1979) Multiple origins of clinopyroxenes in alkali basaltic rocks. *Lithos* 12: 115–132
- Wimmenauer W* (1973) Lamprophyre, Semilamprophyre und anchibasaltische Ganggesteine. *Fortschr Mineral* 51: 3–67
- Witt-Eickschen G, Kaminsky W, Kramm U, Harte B* (1998) The nature of young vein metasomatism in the lithosphere of the West Eifel (Germany): geochemical and isotopic constraints from composite mantle xenoliths from the Meerfelder Maar. *J Petrol* 39: 155–185
- Woolley AR, Bergman SC, Edgar AD, Le Bas MJ, Mitchell RH, Rock NMS, Scott Smith BH* (1996) Classification of lamprophyres, lamproites, kimberlites, and the kalsilitic, melilitic and leucitic rocks. *Can Mineral* 34: 175–186
- Wu B, Berg JH* (1992) Early Paleozoic lamprophyre dikes of southern Victoria Land: geology, petrology and geochemistry. *Antarctic Earth Sci*: 257–264

Authors' addresses: Pr *I. Ngounouno*, Département des Sciences de la Terre, Faculté des Sciences, Université de Ngaoundéré, B.P. 454 Ngaoundéré, Cameroun, e-mail: ngounouno@yahoo.fr; *B. Déruelle* (corresponding author; e-mail: deruelle@ccr.jussieu.fr), Laboratoire de Magmatologie et Géochimie Inorganique et Expérimentale, CNRS-UMR 7047, et IUFM Académie de Versailles, Université Pierre et Marie Curie, 4, place Jussieu, 75252 Paris, Cedex 05, France; *D. Demaiffe*, Laboratoire de Géochimie Isotopique, Université Libre de Bruxelles, 50, Avenue F.D. Roosevelt, CP 160/02, 1050 Bruxelles, Belgique, e-mail: ddemaif@ulb.ac.be; *R. Montigny*, Ecole et Observatoire de Physique du Globe, UMR CNRS 7516, Université Louis Pasteur, 5, rue Descartes, 67100 Strasbourg, France, e-mail: montigny@eopg.u-strasbg.fr